This document is a preprint of: S. Ehsanfar, M. Matthe, D. Zhang et al., "Interference-Free Pilots Insertion for MIMO-GFDM Channel Estimation," in Proceedings of IEEE Wireless Communications and Networking Conference (WCNC 2017), San Francisco, Mar 2017. DOI:10.1109/WCNC.2017.7925957

# Interference-Free Pilots Insertion for MIMO-GFDM Channel Estimation

Shahab Ehsanfar, Maximillian Matthé, Dan Zhang, Gerhard Fettweis, *IEEE Fellow*
Vodafone Chair Mobile Communications Systems
Technische Universität Dresden, Germany
{*firstname.lastname*@ifn.et.tu-dresden.de}

***Abstract*—Generalized Frequency Division Multiplexing (GFDM) is a flexible non-orthogonal waveform. Due to its flexibility it can be served as a framework to emulate diverse multi-carrier waveforms including orthogonal frequency division multiplexing (OFDM) and single-carrier frequency domain equalization (SC-FDE). Nevertheless, depending on the choice of filtering, inter-symbol- and inter-carrier-interference may arise in GFDM. In multiple-input multiple-output (MIMO) scenarios, also inter-antenna-interference further challenges the receiver design. In this paper, we focus on pilot-aided channel estimation for GFDM. In contrast to our prior works, we propose a technique to insert the pilot symbols in a manner such that they are orthogonal to the data symbols in the frequency domain. Based on this design, frequency-domain channel estimation algorithms initially developed for OFDM become straightforwardly applicable. We also examine the impact of such pilot design on the signal properties, including power spectral density (PSD) and peak-to-average-power ratio (PAPR). At the end of the paper, the performance of a MIMO-GFDM system is evaluated and compared with the conventional MIMO-OFDM system.**

## I. Introduction

Modern communication systems demand new requirements that are beyond throughput and data capacity. Low latency applications as in Tactile Internet [1], dynamic spectrum access for cognitive radio and coarse synchronization for smart cities and sporadic traffic have motivated the academia and industrial communities to augment their research on non-orthogonal waveforms [2]. In broadband communications, because of the frequency selectivity, the receiver needs to implement a sophisticated pilot insertion and channel estimation algorithm to properly estimate and equalize the channel effects. Due to the self-interference being generated in non-orthogonal multi-carrier waveforms, the received reference signal (i.e. pilots) is influenced by data symbols. Such impact of the data on pilot symbols degrades the channel estimation performance in comparison to orthogonal frequency division multiplexing (OFDM) which takes advantage of clear pilot observation. Therefore, the OFDM based channel estimations (e.g. [3], [4], [5], etc.) cannot be directly adopted to non-orthogonal waveforms.

Generalized frequency division multiplexing (GFDM) is a well known non-orthogonal waveform being widely researched. Particularly, it has been shown in [6], [7], [8], etc. that the MIMO-GFDM systems have the potential to outperform MIMO-OFDM systems by exploiting the frequency diversity. In this paper, we apply the proposed pilot design for a MIMO-GFDM system. In our prior works [9], [10], [11] on channel estimation for GFDM systems, we needed to handle the data interference on the pilot symbols. The general idea of separating pilot symbols from data symbols has been used in [12]. However, their approach resorts to a precoder calculated based on the knowledge of both data and pilot available at the transmitter. Furthermore, their scheme is only usable for nearly frequency flat fading channels. Our proposal here does not require complicated computation to generate the precoder, while, it is usable for highly frequency selective channels too.

Our contribution in this paper is to modify the GFDM signal for orthogonal pilot insertion and subsequently to achieve an interference-free channel estimation performance for GFDM, though, the approach is applicable to different non-orthogonal multi-carriers which use frequency domain channel estimation as well. Given the low-complexity GFDM transmitter [13], we aim at inserting the pilot subsymbols such that the frequency domain of the receive signal at pilot frequencies have zero influence from data subsymbols. Extracting orthogonal pilots at the receiver side yields an interference-free channel estimation performance. However, due to further modification of the GFDM structure, the transmit signal might have different characteristics compared to the original GFDM signal. Thus, we show the corresponding characteristics of the modified GFDM and accordingly we analyze its receiver performance for a frequency selective MIMO block fading channel while being compared to the original GFDM as well as OFDM.

The rest of this paper is structured as follows: Section II describes the low-complexity frequency domain processing of GFDM and the MIMO channel assumptions. We propose the interference-free pilot insertion (IFPI) technique and its corresponding pilot extraction at the receiver side in Section III. The new signal characteristics in form of peak to average power ratio (PAPR) and out-of-band (OOB) emission as well as further simulation results of the channel estimation and bit error rate (BER) performances based on Monte-Carlo method are provided in Sec. IV. Finally, Sec. V concludes the paper.

### A. Notations

Column-vectors are denoted by vector sign $\vec{X}$ and matrices by boldface $\mathbf{X}$. Time and frequency domain representations are separated by lowercase and uppercase letters, respectively. $\mathbb{E}[\cdot]$ is the expectation operator. The transpose and Hermitian

transpose of $\boldsymbol{X}$ are denoted by $\boldsymbol{X}^T$ and $\boldsymbol{X}^H$, respectively. $\boldsymbol{X} \otimes \boldsymbol{Y}$ and $\boldsymbol{X} \circ \boldsymbol{Y}$ are the Kronecker and Hadamard products [14] of matrices $\boldsymbol{X}$ and $\boldsymbol{Y}$, respectively. $\mathrm{diag}(\vec{X})$ is a diagonal matrix whose diagonal entries are the entries of the column vector $\vec{X}$. Further, $\mathrm{blkdiag}(\boldsymbol{X}, \cdots, \boldsymbol{Y})$ is a block diagonal matrix according to its matrix entries with $\boldsymbol{X}$ being the top-left and $\boldsymbol{Y}$ being the bottom-right blocks. The matrices $\boldsymbol{F}_n$ and $\boldsymbol{I}_n$ are the unitary DFT and the identity matrices of size $n \times n$, respectively. The matrix $\boldsymbol{0}_n$ is an all *zero* matrix of size $n \times n$ while $\boldsymbol{0}_{m \times n}$ has a size of $m \times n$. $\vec{0}_n$ and $\vec{1}_n$ are column vectors of size $n$ with all *zero* and *one* entries, respectively.

## II. GFDM Modulation and System Model

### A. Background

We adopt a GFDM data matrix $\boldsymbol{D} \in \mathbb{C}^{K \times M}$ with $K$ subcarriers and $M$ complex valued subsymbols. The subsymbol at time index $m$ and subcarrier index $k$ is denoted by $d_k[m]$. In GFDM, each data symbol $d_k[m]$ is pulse-shaped using circularly time and frequency shifted version of a prototype filter $g[n]$ whose energy during one period $N = MK$ is normalized to one. Formally, the GFDM transmit sample [15] is given by

$$x[n] = \sum_{k=0}^{K-1} \sum_{m=0}^{M-1} d_k[m] g\big[(n - mK) \bmod N\big] e^{j2\pi \frac{k}{K} n}, \quad (1)$$

with $n = 0, \cdots, N-1$ and $d_k[m] = 0$ if it belongs to an inactive subcarrier. In the above expression, circular filtering is obtained via the modulo operation. Collecting the samples in matrix-vector form, the GFDM transmit signal becomes

$$\vec{x} = \boldsymbol{A}\vec{d}, \quad (2)$$

where $\vec{d} = [\vec{d}_0^T, \cdots, \vec{d}_{K-1}^T]^T \in \mathbb{C}^N$ is vectorized version of $\boldsymbol{D}$ while for each subcarrier $k$ its corresponding $\vec{d}_k$ vector is given by $\vec{d}_k = \big(d_k[m]\big)^T_{(m=0,\cdots,M-1)}$. Moreover, $\vec{d}_k = \vec{\tilde{d}}_k + \vec{\bar{d}}_k$ where $\vec{\tilde{d}}_k$ carries information (consisting both pilots and data) at only pilot subcarriers with zeros at data subcarriers. In a similar fashion, $\vec{\bar{d}}_k$ carries the symbols at data subcarriers including zeros at pilot subcarriers. Hence, $\vec{\tilde{d}}_k \circ \vec{\bar{d}}_k = \vec{0}$ meaning no information between pilot and data subcarriers is superimposed. For future use, we also denote the total number of pilot subcarriers by $K_p = \lfloor K/\Delta k \rfloor$ with $\Delta k$ being the pilot subcarrier spacing. Likewise, $K_d = K - K_p$ is the total number of data subcarriers. The modulation matrix is denoted by $\mathbf{A}$ and it consists of all necessary signal processing operations.

Next, we write the equivalent version of (2) for the signal associated to the data subcarriers as [13]

$$\vec{\tilde{x}} = \boldsymbol{F}_N^H \sum_{k=0}^{K-1} \boldsymbol{P}^{(k)} \boldsymbol{G}^{(\delta)} \boldsymbol{R}^{(\delta)} \boldsymbol{F}_M \vec{\tilde{d}}_k, \quad (3)$$

where $\boldsymbol{R}^{(\delta)}$ is $\delta$-fold repetition matrix which concatenates $\delta$ identity matrices $\boldsymbol{I}_M$ of size $M$ i.e. $\boldsymbol{R}^{(\delta)} = (\boldsymbol{I}_M \ \boldsymbol{I}_M \ \cdots)^T$. The value of $\delta$ is based on the number of non-zero values in filter frequency response e.g. if a filter spans over two subcarriers $\delta$ is typically selected as $\delta = 2$. In (3) due to the circular filtering, the subcarrier filter $\boldsymbol{G}^{(\delta)} = \mathrm{diag}(\vec{G}^{(\delta)})$ is diagonal in frequency domain with $\vec{G}^{(\delta)} = \boldsymbol{F}_{M\delta} \vec{g}^{(\delta)}$. The circulant filter $\vec{g}^{(\delta)}$ is the down-sampled version of $\vec{g} = \big(g[n]\big)_{n=0,\cdots,N-1}$ by factor $K/\delta$. The permutation matrix $\boldsymbol{P}^{(k)}$ shifts the DC signals to their corresponding subcarriers (i.e. $k$) and is given by

$$\boldsymbol{P}^{(k)} = \boldsymbol{C}_\ell \begin{bmatrix} \boldsymbol{0}_{M\delta/2} & \boldsymbol{I}_{M\delta/2} & \boldsymbol{0}_{M\delta/2 \times (N-\delta M)} \\ \boldsymbol{I}_{M\delta/2} & \boldsymbol{0}_{M\delta/2} & \boldsymbol{0}_{M\delta/2 \times (N-\delta M)} \end{bmatrix}^T, \quad (4)$$

where $\ell = kM - M\delta/2$. The circulant matrix $\boldsymbol{C}_\ell$ follows:

$$\boldsymbol{C}_\ell = \mathrm{circ}([\vec{0}^T_{\ell \bmod N}, \ 1, \ \vec{0}^T_{(N-\ell-1) \bmod N}]), \quad (5)$$

here, $\mathrm{circ}(\cdot)$ returns a circulant matrix associated to its input row vector.

### B. MIMO Channel

We consider a multipath MIMO block fading channel with $\mathsf{n_T}$ transmit (Tx) and $\mathsf{n_R}$ receive (Rx) antennas. At the Tx antenna $i_\mathsf{T}$, the signal is modulated using GFDM and then protected by a cyclic prefix (CP). We assume that all the channels have shorter lengths $L$ than the CP length. Thus, the receive signal after CP removal at Rx antenna $i_\mathsf{R}$ is characterized by the following equation:

$$\vec{y}_{i_\mathsf{R}} = \sum_{i_\mathsf{T}=1}^{\mathsf{n_T}} \vec{x}_{i_\mathsf{T}} \circledast \vec{h}_{i_\mathsf{T}, i_\mathsf{R}} + \vec{w}_{i_\mathsf{R}}, \quad (6)$$

where $\circledast$ denotes the circular convolution of the channel impulse response $\vec{h}_{i_\mathsf{T}, i_\mathsf{R}}$ and the transmit signal $\vec{x}_{i_\mathsf{T}}$. Further, $\vec{w}_{i_\mathsf{R}}$ is the vector of additive white Gaussian noise (AWGN) samples with variance $\sigma_w^2$ received at antenna $i_\mathsf{R}$.

In DFT domain, circular convolution turns into multiplication and therefore, the observed signal on Rx antenna $i_\mathsf{R}$ is given by

$$\vec{Y}_{i_\mathsf{R}} = \sum_{i_\mathsf{T}=1}^{\mathsf{n_T}} \boldsymbol{X}_{i_\mathsf{T}} \vec{H}_{i_\mathsf{T}, i_\mathsf{R}} + \vec{W}_{i_\mathsf{R}}, \quad (7)$$

where $\vec{H}_{i_\mathsf{T}, i_\mathsf{R}} = \sqrt{N} \mathbf{F}_{N \times L} \vec{h}_{i_\mathsf{T}, i_\mathsf{R}}$ and $\mathbf{F}_{N \times L} \subset \mathbf{F}_N$ consists of the first $L$ columns of $\mathbf{F}_N$. The diagonal matrix $\boldsymbol{X}_{i_\mathsf{T}} = \mathrm{diag}(\mathbf{F}_N \vec{x}_{i_\mathsf{T}})$ and the vector $\vec{W}_{i_\mathsf{R}} = \mathbf{F}_N \vec{w}_{i_\mathsf{R}}$ are the frequency counterparts of the transmit signal and the received noise respectively.

## III. Interference-free pilot insertion

### A. Pilot transmission

In this section, in contrast to the approach used in [9] and [10], we aim to insert orthogonal pilots into the pilot subcarriers. In GFDM modulation, it is possible to reserve some frequency bins specifically for the pilots without any influence from the data symbols. Thus, we modify the expression (3) by the following:

$$\vec{x} = \boldsymbol{F}_N^H \sum_{k=0}^{K-1} \boldsymbol{P}^{(k)} \boldsymbol{G}^{(\delta)} \boldsymbol{R}^{(\delta)} \left( \boldsymbol{\Gamma} \vec{\tilde{d}}_k + \boldsymbol{F}_M \vec{\bar{d}}_k \right), \quad (8)$$

where $\boldsymbol{\Gamma} = \boldsymbol{P'} \mathrm{blkdiag}(\lambda \boldsymbol{I}_{\mathsf{n_T}}, \boldsymbol{F}_{M-\mathsf{n_T}})$. Here, $\boldsymbol{P'}$ can be any permutation matrix of compatible size which allocates the

This document is a preprint of: S. Ehsanfar, M. Matthe, D. Zhang et al., "Interference-Free Pilots Insertion for MIMO-GFDM Channel Estimation," in Proceedings of IEEE Wireless Communications and Networking Conference (WCNC 2017), San Francisco, Mar 2017. DOI:10.1109/WCNC.2017.7925957

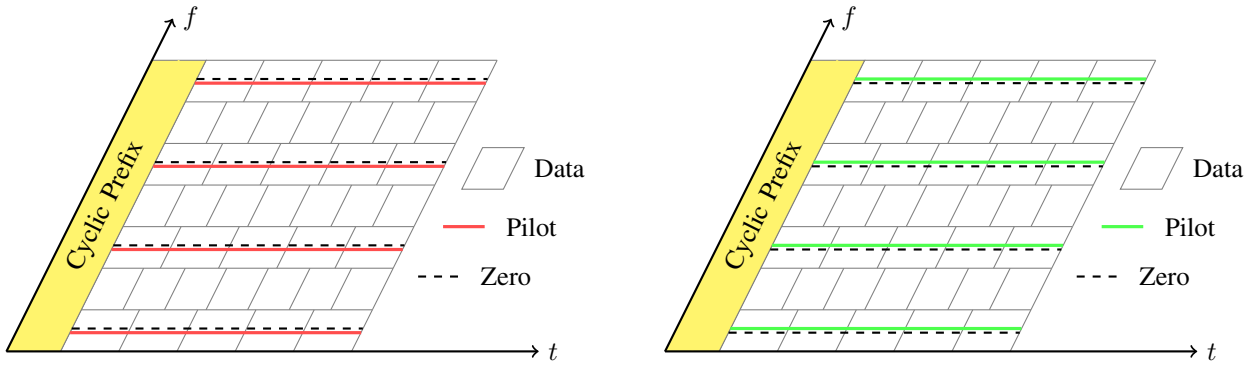


(a) Antenna 1 (b) Antenna 2

Fig. 1: Pilots and Data subsymbols in time-frequency resources

pilots to any frequency bin within the pilot subcarriers. The parameter $\lambda$ is a scaling factor that normalizes the pilots energy to one. Note that in expression (8) the plus sign does not superimpose the information i.e. if $k$ is a pilot subcarrier $\boldsymbol{F}_M\vec{d}_k$ becomes $\vec{0}_M$ and if it belongs to data subcarriers $\boldsymbol{\Gamma}\vec{d}_k$ would be $\vec{0}_M$. Additionally, the signal $\vec{\tilde{x}}$ at pilot subcarriers can be obtained from the first term of Eq. (8) i.e.

$$\vec{\tilde{x}} = \boldsymbol{F}_N^H \sum_{k=0}^{K-1} \boldsymbol{P}^{(k)}\boldsymbol{G}^{(\delta)}\boldsymbol{R}^{(\delta)}\boldsymbol{\Gamma}\vec{\tilde{d}}_k. \tag{9}$$

In Eq. (9), if as an example, we set $\boldsymbol{P}' = \boldsymbol{I}_M$, the first $\mathsf{n_T}$ subsymbols of the pilot subcarriers (i.e. $\{\tilde{d}_k[0], \tilde{d}_k[1], \cdots, \tilde{d}_k[\mathsf{n_T}-1]\}$ which are filled with pilots) are processed directly in frequency domain being isolated from the rest of subsymbols. Although, such isolation holds if and only if the pilots are located at the frequency bins where no inter-carrier interference is present. In this case, each orthogonal subsymbol can be reserved for a specific Tx antenna such that the $\mathsf{n_T} \times \mathsf{n_R}$ MIMO channel can be processed in terms of $\mathsf{n_T}\mathsf{n_R}$ single-input single-output (SISO) channels. The approach can be considered as a variation of cell-specific reference signal mapping in LTE [16]. Fig. 1 shows an example how the pilot subsymbols in the GFDM data block are mapped into the time-frequency grid of the resources for a $2 \times 2$ MIMO channel. Here, two frequency bins of the pilot subcarriers are reserved only for the pilots while at each Tx antenna only one pilot is being transmitted. Thus, the pilot is being transmitted during the whole GFDM symbol, while also the energies of the data subsymbols are no longer concentrated at equally spaced $M$ peaks. Fig. 2 shows an example of the signal filtering in frequency domain where the pilots at different antennas are orthogonal to one another as well as to the data samples.

### B. Received pilots

Since the pilots from each Tx antenna are orthogonal to the rest of subsymbols, the channel between each Tx-Rx antenna pair can be separately estimated using the existing estimation techniques. For such separate estimations, we need to extract the pilot frequencies from the received signal at each

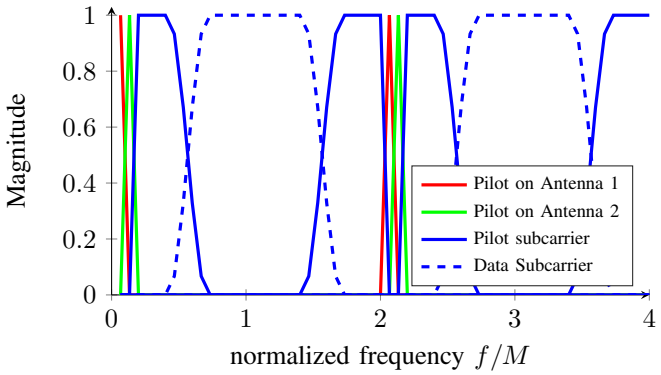


Fig. 2: Signal spectrum for $M = 15$ , $K = 4$, $\boldsymbol{P}' = \boldsymbol{I}_M$

Rx antenna. Define the matrix $\boldsymbol{F}^{(i_\mathsf{T})} \subset \boldsymbol{F}_N$ which contains only the rows of the DFT matrix associated to the frequency bins of the pilots from antenna $i_\mathsf{T}$. The matrix $\boldsymbol{F}^{(i_\mathsf{T})}$ yields to non-zero values in frequency domain of the pilots signal $\vec{X}'_{i_\mathsf{T}} = \boldsymbol{F}^{(i_\mathsf{T})}(\vec{\tilde{x}}_0)_{i_\mathsf{T}}$ from antenna $i_\mathsf{T}$. Here, $\vec{\tilde{x}}_0$ is a known time domain pilots signal and it is generated in a similar fashion as $\vec{\tilde{x}}$ (i.e. Eq. (9)) with the only difference that zeros are inserted at data positions of $\vec{\tilde{d}}_k$. Due to $\boldsymbol{F}^{(i_\mathsf{T})}$, also the frequency domain signal $\vec{X}_{i_\mathsf{T}} = \boldsymbol{F}^{(i_\mathsf{T})}\vec{x}_{i_\mathsf{T}}$ consists only pilot values (of antenna $i_\mathsf{T}$) with zero influence from data subsymbols.

Once the DFT matrix $\boldsymbol{F}^{(i_\mathsf{T})}$ associated to the frequencies of interest is specified, the signal due to the received pilots from Tx antenna $i_\mathsf{T}$ at Rx antenna $i_\mathsf{R}$ is given by

$$\vec{Y}_{i_\mathsf{T},i_\mathsf{R}} = \boldsymbol{F}^{(i_\mathsf{T})}\vec{y}_{i_\mathsf{R}}. \tag{10}$$

Here, since each received pilot sequence $\vec{Y}_{i_\mathsf{T},i_\mathsf{R}}$ between antenna pairs $i_\mathsf{T}$-$i_\mathsf{R}$ can be treated separately in form of multiple SISO channels, we refer the readers to [10] for the least squares (LS) and linear minimum mean square error (LMMSE) estimations of the channel.

### C. Complexity

Due to the orthogonality of the pilots and data in frequency domain, the complexity of the channel estimation for IFPI

This document is a preprint of: S. Ehsanfar, M. Matthe, D. Zhang et al., "Interference-Free Pilots Insertion for MIMO-GFDM Channel Estimation," in Proceedings of IEEE Wireless Communications and Networking Conference (WCNC 2017), San Francisco, Mar 2017. DOI:10.1109/WCNC.2017.7925957

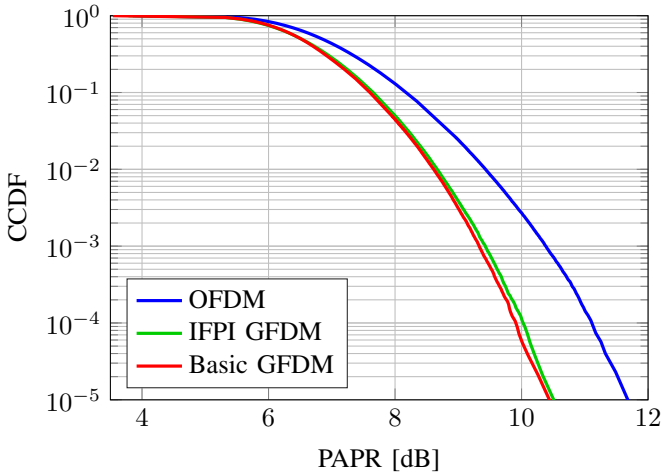


Fig. 3: Signal PAPR for $M = 21$ , $K = 4$ vs. its complementary cumulative distribution function (CCDF)

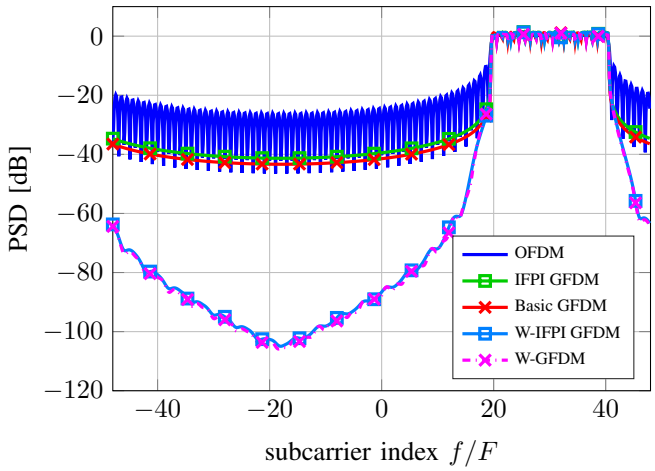


Fig. 4: Out of band emission for $K = 96$, $M = 15$ and the total number of frequency samples $F$

GFDM turns out to be identical to that of OFDM and hence, it becomes less complex than the channel estimation in basic GFDM. In basic GFDM, since the interference from data subsymbols is treated as extra correlated noise, further signal processing operations are required to reduce the impact of such interference. Moreover, since the pilots are spread over all frequency bins of the pilot subcarriers, more frequency domain pilot samples (i.e. $N_p = K_p M$ samples) need to be handled in basic GFDM. Considering the matrix inversion in LMMSE estimator, the complexity of channel estimation in OFDM as well as IFPI GFDM is proportional to $\mathcal{O}(\mathsf{n_T n_R} K_p^3)$ whereas the basic GFDM requires $\mathcal{O}(\mathsf{n_R} N_p^3)$ operations for its LMMSE channel estimation. On the other hand, since the IFPI GFDM employs the frequency domain GFDM modulation for orthogonal pilot insertion, its complexity increases with respect to the basic GFDM modulated in time domain. The time domain GFDM modulation [17] requires an implementation effort of $M(N + K \log_2 K)$ in terms of number of complex multiplications. The frequency domain GFDM modulation needs $N \log_2 N + K\delta M + KM \log_2 M$ complex multiplications [13]. Though, for IFPI GFDM it slightly reduces to $N \log_2 N + K\delta M + K_p(M - \mathsf{n_T}) \log_2(M - \mathsf{n_T}) + K_d M \log_2 M$. In general, considering a receiver that employs a channel estimator, the complexity of the data transmission in IFPI GFDM becomes smaller than that of basic GFDM with the channel estimation proposed in [9].

## IV. Simulation Results

In order to evaluate the performance of GFDM with interference-free pilot design, we adopt a $2 \times 2$ MIMO block fading multipath channel with Rayleigh distribution. Here, by considering the performance of OFDM channel estimation as a benchmark, we compare the performance of GFDM under the impact of channel estimation with the proposed orthogonal pilot insertion versus the prior works [9], [10] which adapted the basic GFDM pilot insertion. The PAPR, OOB radiation, mean squared error (MSE) and the coded BER performances are evaluated through Monte-Carlo simulations with the parameters summarized in Table I. The signal to noise ratio is denoted by $\mathcal{E}_s/N_0$ and considering also the coding gain we have $\mathcal{E}_b/N_0 = \mathcal{E}_s/N_0 - 10\log_{10}(\mu r)$ where $\mu$ and $r$ denote the modulation order and the code-rate respectively. The received signal constellations are detected via GFDM zero forcing demodulation and MMSE frequency domain equalization i.e. $\hat{\vec{d}} = (\boldsymbol{I}_{\mathsf{n_R}} \otimes \boldsymbol{A}^{-1})\boldsymbol{Q}[\vec{Y}_1^T \ \cdots \ \vec{Y}_{\mathsf{n_R}}^T]^T$, where, $\boldsymbol{Q} = (\hat{\boldsymbol{H}}^H \hat{\boldsymbol{H}} + \sigma_w^2 \boldsymbol{I}_N)^{-1} \hat{\boldsymbol{H}}^H$ is the equalization matrix using the estimated channels matrix $\hat{\boldsymbol{H}}$. The detected data symbols are transferred into maximum likelihood (ML) symbol log-likelihoods and they are then fed into the soft demapper with 8 turbo decoder iterations.

| *Parameter* | *Symbol* | *GFDM* | *OFDM* |
|---|---|---|---|
| Modulation order | $\mu$ | 4 (16-QAM) | |
| No. of subsymbols | $M$ | 7,15,21 | 1 |
| No. of subcarriers | $K$ | 4,96 | 84, 96, 672 |
| Pilot subcarrier spacing | $\Delta k$ | 3 | 21 |
| Roll-off factor of RC filter | $\alpha$ | 0.3 | 0 |
| GFDM demodulation | - | Zero Forcing | - |
| Pilot sequence - Basic [9] | - | Complex randoms | - |
| Pilot sequence - IFPI, OFDM | - | $1^{\text{st}}$ root Zadoff-Chu | |
| Channel equalization | - | MMSE | |
| Channel coding | - | Parallel Concatenated Convolutional Codes | |
| Octal generator polynomial | - | (1,15/13) | |
| Decoder decision metric | - | log-MAP | |
| No. of turbo iterations | - | 8 | |
| No. of channel taps | $L$ | 24 | |
| Power delay profile | - | Exponential | |

TABLE I: Simulation Parameters

The PAPR of the proposed signal is compared to the original GFDM beside OFDM in Fig. 3. One can see that due to orthogonal pilot insertion, the PAPR of IFPI GFDM increases with respect to the basic GFDM. However, it still has more than one dB difference with the PAPR of an OFDM signal.

This document is a preprint of: S. Ehsanfar, M. Matthe, D. Zhang et al., "Interference-Free Pilots Insertion for MIMO-GFDM Channel Estimation," in Proceedings of IEEE Wireless Communications and Networking Conference (WCNC 2017), San Francisco, Mar 2017. DOI:10.1109/WCNC.2017.7925957

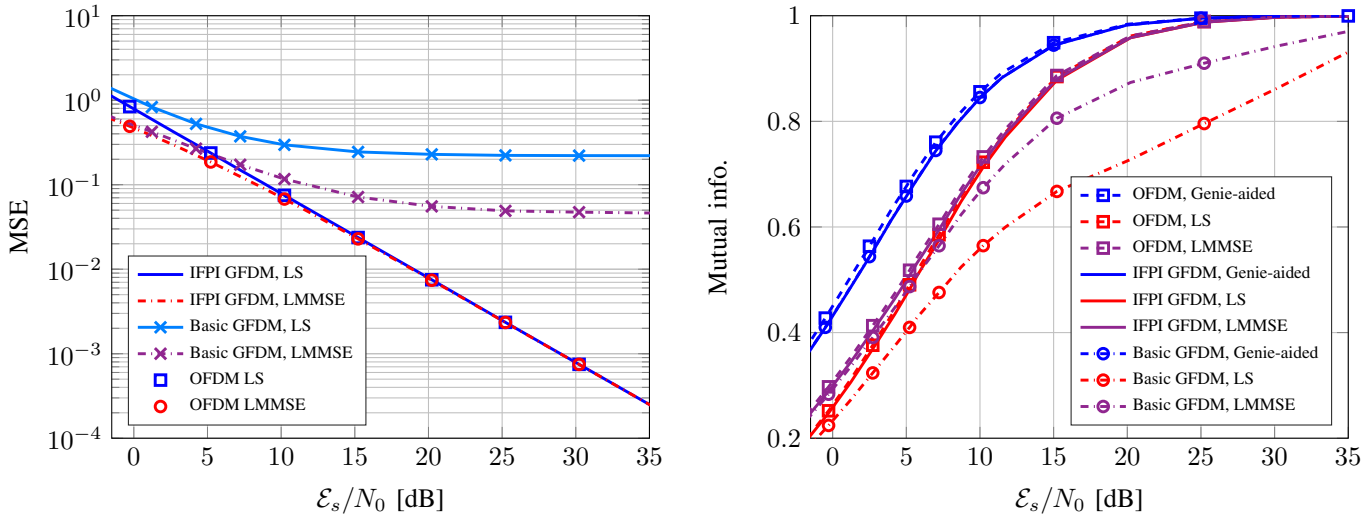


(a) Channel estimation performance for $M = 7, K = 96$

(b) Mutual information of transmitted bitstream vs received bit LLRs for $M = 7, K = 96$ (after encoder and before decoder)

Fig. 5: MSE and MI Performances with 5% pilots overhead over $2 \times 2$ MIMO channel

On the other hand, comparing the power spectral densities of the signals in Fig. 4, we observe that, despite IFPI GFDM has slightly larger OOB compared to the original GFDM signal, the windowed case achieves almost the same OOB radiation as in original windowed GFDM (W-GFDM). The window function is configured in form of Raised Cosine (RC) window with a ramp length of a quarter subsymbol. For further details regarding the windowing process, we refer the interested readers to [15].

Figure 5a compares the MSE performances of channel estimation with the proposed IFPI technique, OFDM and the basic GFDM channel estimation [9]. Due to the orthogonality of the pilots to the data symbols in IFPI, one can see that the performance of such channel estimation becomes identical with the performance of OFDM. However, the basic GFDM channel estimation which suffers from significant interference has a large error floor at high signal to noise ratio (SNR) regions. Similar behavior can also be observed in Fig. 5b. The genie-aided receivers have perfect knowledge of the channel state information without transmitting pilots. Here, the OFDM genie-aided receiver has slightly larger mutual information with respect to the both GFDM cases due to the orthogonality between the data symbols. With the current GFDM configuration the self-interference is treated as extra noise at the receiver slightly limiting its outcome, although, such performance loss is marginal when we consider the GFDM gains in PAPR and OOB emission. Also note that the genie-aided receiver of IFPI GFDM has slightly smaller mutual information with respect to the basic GFDM genie-aided receiver which is due to the fact that in basic GFDM the energies of the data subsymbols are spread over all frequency bins of the pilot subcarriers gaining more frequency diversity. However, if we employ the channel estimation, IFPI GFDM achieves a significant gain with respect to basic GFDM. Because of the interference from data symbols in basic GFDM channel estimation, full information transfer cannot be achieved even at high SNR regions. On the other hand, IFPI GFDM with imperfect channel knowledge (e.g. LS and LMMSE estimations) follow the OFDM performance with slight difference.

The coded performances of the three receiver types are provided in Fig. 6. Employing a robust code-rate of 1/3, OFDM, IFPI GFDM and basic GFDM receivers obtain almost similar BER, though, basic GFDM with LS estimation has 2-3 dB worse BER performance than the rest of receivers with imperfect channel knowledge. Here, due to around 1 dB gap of the genie-aided receivers of OFDM and IFPI GFDM, the latter receiver stays around 0.5 dB behind OFDM when the channel is estimated through pilot transmission. On the other hand, Fig. 6b shows that the basic GFDM channel estimation with non-orthogonal pilots becomes entirely unqualified for a high code-rate of 5/6 which is due to its large error floor in channel estimation. Comparing OFDM and IFPI GFDM, we observe that the performance loss in GFDM which is a non-orthogonal waveform is not significant compared to OFDM. Furthermore, in Fig. 6b the BER for LS and LMMSE estimations in OFDM as well as IFPI GFDM are identical due to identical channel estimation performances at high SNR regions.

## V. Conclusion

This paper proposed an interference-free pilot insertion technique for channel estimation in a non-orthogonal multi-carrier system. Although, the approach is applied to MIMO-GFDM, it is applicable to other non-orthogonal waveforms with frequency domain channel estimation as well. Here, the coded performances of different GFDM receivers were evaluated and compared to the performance of OFDM with imperfect channel knowledge. From simulation results we observed that IFPI GFDM achieves identical channel estimation

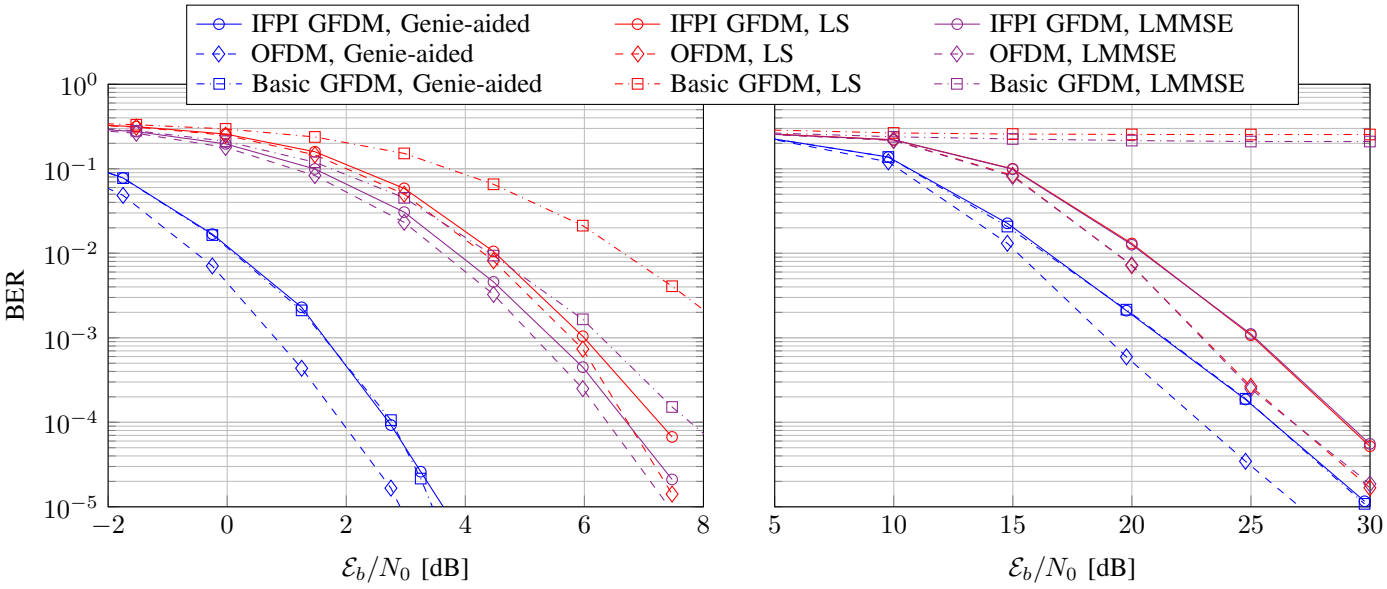


(a) 1/3 code-rate

(b) 5/6 code-rate

Fig. 6: Bit Error Rate performance for 5% pilots overhead over $2 \times 2$ MIMO channel ($M = 7, K = 96$)

performance as in OFDM which significantly outperforms the prior works on GFDM channel estimation [9], [10] at high SNRs. The simulation of bit error rate performances of different GFDM receivers with imperfect channel knowledge shows that IFPI GFDM can achieve comparable results with OFDM while the basic pilot insertion for GFDM was subject to appreciable performance loss for high code-rates. In the future, we would be interested to apply the GFDM channel estimation to more challenging scenarios such as highly doubly dispersive channels. In [6], GFDM was shown to outperform OFDM in terms of exploiting the frequency selectivity. A potential future work could be to compare the performance of both waveforms in terms of harnessing the time selectivity.

## ACKNOWLEDGMENT

The computations were performed at the Center for Information Services and High Performance Computing (ZIH) of TU Dresden. The work presented in this paper has been performed in the framework of the SATURN project with contract no. 100235995 funded by the Europäischer Fonds für regionale Entwicklung (EFRE). Part of this work is also sponsored by the Federal Ministry of Education and Research within the program "Twenty20 - Partnership for Innovation" contract no. 03ZZ0505B - "Fast Wireless".

## REFERENCES

[1] G. Fettweis, "The Tactile Internet: Applications and Challenges," *IEEE Veh. Technol. Mag.*, vol. 9, no. 1, pp. 64–70, 2014.

[2] G. Wunder, P. Jung, M. Kasparick, T. Wild, F. Schaich, Y. Chen, S. Brink, I. Gaspar, N. Michailow, A. Festag *et al.*, "5GNOW: non-orthogonal, asynchronous waveforms for future mobile applications," *IEEE Commun. Mag.*, vol. 52, no. 2, pp. 97–105, 2014.

[3] S. Coleri, M. Ergen, A. Puri, and A. Bahai, "Channel estimation techniques based on pilot arrangement in OFDM systems," *IEEE Trans. Broadcast.*, vol. 48, no. 3, pp. 223–229, 2002.

[4] M. Biguesh and A. Gershman, "MIMO channel estimation: optimal training and tradeoffs between estimation techniques," in *Proc. IEEE Int. Conf. on Commun.*, vol. 5, 2004, pp. 2658–2662 Vol.5.

[5] G. Taricco and G. Coluccia, "Optimum Receiver Design for Correlated Rician Fading MIMO Channels with Pilot-Aided Detection," *IEEE J. Sel. Areas Commun.*, vol. 25, no. 7, pp. 1311–1321, 2007.

[6] D. Zhang, L. Mendes, M. Matthé, I. Gaspar, N. Michailow, and G. Fettweis, "Expectation Propagation for Near-Optimum Detection of MIMO-GFDM Signals," *IEEE Trans. Wireless Commun.*, 2015.

[7] M. Matthé, D. Zhang, and G. Fettweis, "Iterative Detection using MMSE-PIC Demapping for MIMO-GFDM Systems," in *Proc. of the EW European Wireless Conference (EW'16)*. IEEE, 2016.

[8] M. Matthé, L. Mendes, N. Michailow, D. Zhang, and G. Fettweis, "Widely Linear Estimation for Space-Time-Coded GFDM in Low-Latency Applications," *IEEE Trans. Commun.*, 2015.

[9] S. Ehsanfar, M. Matthé, D. Zhang, and G. Fettweis, "A Study of Pilot-Aided Channel Estimation in MIMO-GFDM Systems," in *Proc. of the ITG/IEEE Workshop on Smart Antennas (WSA'16)*, 2016.

[10] S. Ehsanfar, M. Matthe, D. Zhang, and G. Fettweis, "Theoretical Analysis and CRLB Evaluation for Pilot-aided Channel Estimation in GFDM," in *Proc. of the IEEE Global Communications Conference (GLOBECOM'16)*, 2016.

[11] M. Danneberg, N. Michailow, I. Gaspar, M. Matthé, D. Zhang, L. L. Mendes, and G. Fettweis, "Implementation of a 2 by 2 MIMO-GFDM Transceiver for Robust 5G Networks," in *Proc. of the Twelfth Int. Symposium on Wireless Commun. Syst. (ISWCS'15)*, 2015.

[12] U. Vilaipornsawai and M. Jia, "Scattered-pilot channel estimation for GFDM," in *Proc. IEEE Wireless Commun. and Netw. Conf. (WCNC)*, 2014, pp. 1053–1058.

[13] I. Gaspar, N. Michailow, A. Navarro, E. Ohlmer, S. Krone, and G. Fettweis, "Low complexity GFDM receiver based on sparse frequency domain processing," in *Vehicular Technology Conference (VTC Spring), 2013 IEEE 77th*. IEEE, 2013, pp. 1–6.

[14] A. H. Roger and R. J. Charles, "Topics in matrix analysis," 1991.

[15] N. Michailow et. al., "Generalized Frequency Division Multiplexing for 5th Generation Cellular Networks," *IEEE Trans. Commun.*, vol. 62, no. 9, pp. 3045–3061, 2014.

[16] E. U. T. R. Access, "Physical channels and modulation," *3GPP TS*, vol. 36, p. V8, 2009.

[17] M. Matthé, L. Mendes, I. Gaspar, N. Michailow, D. Zhang, and G. Fettweis, "Precoded GFDM transceiver with low complexity time domain processing," *EURASIP Journal on Wireless Communications and Networking*, vol. 2016, p. 138, 2016.